Wind and Structures, *Vol. 26, No. 1 (2018) 35-43*
DOI: https://doi.org/10.12989/was.2018.26.1.035

Numerical investigation of truck aerodynamics on several classes of infrastructures

Alejandro Alonso-Estébanez[*1], Juan J. del Coz Díaz[2], Felipe P. Álvarez Rabanal[2], Pablo Pascual-Muñoz[1] and Paulino J. García Nieto[3]

[1]*Department of Transport, Projects and Process Technology, University of Cantabria, Avda. Los Castros s/n, 39005 Santander, Spain*
[2]*Department of Construction, GICONSIME Research Team, University of Oviedo, Departmental Building 7, 33204 Gijón, Spain*
[3]*Department of Mathematics, Faculty of Sciences, University of Oviedo, 33007 Oviedo, Spain*

(Received September 26, 2017, Revised December 29, 2017, Accepted January 4, 2018)

Abstract. This paper describes the effect of different testing parameters (configuration of infrastructure and truck position on road) on truck aerodynamic coefficients under cross wind conditions, by means of a numerical approach known as Large Eddy Simulation (LES). In order to estimate the air flow behaviour around both the infrastructure and the truck, the filtered continuity and momentum equations along with the Smagorinsky–Lilly model were solved. A solution for these non-linear equations was approached through the finite volume method (FVM) and using temporal and spatial discretization schemes. As for the results, the aerodynamic coefficients acting on the truck model exhibited nearly constant values regardless of the Reynolds number. The flat ground is the infrastructure where the rollover coefficient acting on the truck model showed lowest values under cross wind conditions (yaw angle of 90º), while the worst infrastructure studied for vehicle stability was an embankment with downward-slope on the leeward side. The position of the truck on the road and the value of embankment slope angle that minimizes the rollover coefficient were determined by successfully applying the Response Surface Methodology.

Keywords: cross wind; embankments; heavy vehicles aerodynamics; Large Eddy Simulation (LES); Finite Volume Method (FVM); Computational Fluid Dynamics (CFD)

1. Introduction

As a consequence of cross wind induced accidents in road/rail transportation, the amount of research on this issue has increased over the last years (Baker and Reynolds 1992, Bettle *et al*. 2003, Bocciolone *et al*. 2008). Several accidents due to cross wind have been registered and analysed worldwide (Coleman and Baker 1990, Imai et al. 2002, Shao *et al*. 2011). High-sided vehicles such as trucks, caravans and trains are especially affected by cross wind since the risk of rollover is higher than for other kinds of vehicles (Dorigatti *et al*. 2012). In addition, new vehicles are designed to be lighter to reduce their energy consumption and this aspect negatively affects their stability during driving (Alvarez-Legazpi *et al*. 2010).

The overturning risk associated with cross wind mainly depends on local wind characteristics and the dynamic behavior of vehicles. The local wind characteristics are influenced by the infrastructure scenario along transportation routes (Suzuki *et al*. 2003, Cheli *et al*. 2010). At locations such as embankments, bridges and tunnel exits, vehicles have more susceptibility to rollover than in other places. Therefore, better knowledge of the stability of vehicles by measuring the aerodynamic coefficients in these scenarios may improve the safety regulations in cross wind conditions.

For this reason, several methodologies have been used by different researchers to analyze the stability of high-sided vehicles under cross wind conditions in these risky infrastructures.

Dorigatti *et al.* (2012) carried out wind tunnel tests to obtain the aerodynamic loads of three kinds of vehicles located on two models of bridge. Other research has been focused on vehicle stability in special bridge locations such as bridge towers (Argentini *et al*. 2011, Ma *et al.* 2016, Wu *et al.* 2017). This is because the towers cause sudden changes in the aerodynamic loads of the vehicles. Moreover, the effect of embankments on the overturning risk of vehicles has been analyzed in several studies (Diedrichs *et al.* 2007, Miao *et al.* 2010, Schober *et al.* 2010) due to the wind speed increasing on upslopes (Bitsuamlak et al. 2004).

This knowledge of unstable aerodynamic loads acting on vehicles for different scenarios has been used for the development of wind warning systems to protect high-speed trains against strong cross winds (Hoppmann *et al*. 2002, Delaunay *et al*. 2006). Other studies focus on the optimization of barriers to improve the protection of vehicles against cross wind conditions (Yang *et al*. 2017). So far, different techniques such as numerical simulation, wind tunnel testing and full scale experiments have been used to evaluate vehicle stability under cross wind conditions. For instance, Hibino *et al.* (2010) carried out a full-scale experiment to validate the equation that is applied to solve the overturning problem of a rigid body. Wind

*Corresponding author, Ph.D.
E-mail: alonsoea@unican.es

ISSN: 1226-6116 (Print), 1598-6225 (Online)

tunnel tests were performed by Bocciolone *et al.* (2008) to analyze the most critical conditions in several road infrastructures as a result of cross wind action. Sterling *et al.* (2010) contrasted the results of aerodynamic loads acting on a truck by using the three techniques cited above.

In this paper, the aerodynamic coefficients of a truck model in different scenarios and subjected to cross wind conditions are obtained by means of numerical simulation. This study aims to analyze how different configurations of embankments affect vehicle stability by using a validated numerical model in combination with a design of experiments (DOE) methodology. This methodology enables scenarios to be distinguished in which risk of rollover accident due to cross wind action is especially relevant. This information can be very useful for making relevant decisions in terms of traffic safety improvement (use of wind fences, new regulations, etc.). Moreover, a better understanding of how different geometric parameters of embankments affect the aerodynamics of the vehicle can be very valuable for the design of road structures with reduced risk of rollover accidents. The first section of the paper describes the CFD model and its numerical setup while the second analyzes the results provided by the numerical simulation. Finally, the most important conclusions are drawn based on the results obtained.

2. Numerical procedure

2.1 Mathematical approach

Cross winds that negatively influence vehicle stability are characterized by a turbulent regime, which consists of eddies with a wide range of length and time scales. It is possible to solve the whole spectrum of turbulent scales by applying the method known as direct numerical simulation (DNS). However, the high computational cost required to solve common engineering problems by using the DNS approach makes this unfeasible (ANSYS FLUENT 2017). With another approach known as Large Eddy Simulation (LES) only large eddies are solved directly whereas the small eddies are solved using turbulence models. Therefore, LES enables the use of coarser grids and larger time steps in comparison to DNS, as well as finer grids than those used in models solved with the Reynolds-Averaged Navier–Stokes equations approach (RANS). All turbulent scales are modeled in RANS; therefore, LES allows more accurate results to be obtained than RANS, particularly for cases where significant unsteadiness in the large scale of flow are generated, as could happen around trucks under cross wind conditions. Accordingly, the LES approach was used to carry out the 3D numerical simulation presented in this work. The LES approach was also used in other studies to analyze the effect of cross wind conditions on the stability of vehicles such as cars and trains (Tsubokura *et al.* 2010, García *et al.* 2015, Dragomirescu *et al.* 2016).

The LES approach filters the Navier-Stokes equations and resolves these equations for the large-scale eddies. The filtered continuity and momentum equations for an incompressible flow are

$$\frac{\partial}{\partial x_i}\left(\rho \bar{u}_i\right)=0 \tag{1}$$

$$\frac{\partial}{\partial t}\left(\rho \bar{u}_i\right)+\frac{\partial}{\partial x_j}\left(\rho \bar{u}_i \bar{u}_j\right)=\frac{\partial}{\partial x_j}\left(\sigma_{ij}\right)-\frac{\partial \bar{p}}{\partial x_i}-\frac{\partial \tau_{ij}}{\partial x_j} \tag{2}$$

where $\bar{u}_i$ and $\bar{p}$ are the filtered component of velocity in the *i* direction and pressure, respectively; σ_{ij} is the stress tensor due to molecular viscosity; and τ_{ij} is the subgrid-scale turbulent stress tensor. In order to obtain the term τ_{ij}, the Boussinesq assumption was considered and the Smagorinsky–Lilly model (Smagorinsky 1963) was employed. Detailed information about these equations can be found in ANSYS FLUENT (2017).

The finite volume method (FVM) is applied to solve the equations described above, which detail the transport of the main properties of turbulent flow. The geometric domain is divided into a finite number of cells with nodal points. The virtual control volumes are cell-centered and are directly delimited by the grid nodes, and the variables' values will only be available at the center of cells. The governing equations that describe the conservation of a general variable of flow ϕ (e.g., components of the flow velocity *u*, or pressure) are integrated within the control volumes.

In this research work, a bounded second-order implicit scheme was used for time discretization. Regarding spatial discretization, the following schemes were used: Least Squares Cell-Based to calculate gradients; second order to calculate the pressure gradient term; and bounded central differencing to solve the convection-diffusion equations. The SIMPLE algorithm of Patankar and Spalding (1972) was used to solve pressure–velocity coupling. This is a recommended configuration for single-phase problems using either the pressure-based or density-based solver (ANSYS FLUENT 2017). The time step was set based on the ratio between the vehicle width and the upstream wind velocity obtained at the level of the vehicle (Wang 2014). Therefore, the time step was defined as

$$\Delta t = 0.1\frac{W}{U} \tag{3}$$

where *W* is the width of vehicle and *U* is the upstream wind velocity. The Courant–Friedrichs–Lewy number (CFL) was below one in most of the cells for the time step used. The flow covered three times the domain before the results were sampled. The aerodynamic coefficients were averaged during 2300Δt, which is the time required by the air flow to cover three times the domain.

Finally, the algebraic equation system was solved by using an iterative method. A converged solution was reached when the following requirements were met (ERCOFTAC 2000): scaled residuals of all the variables below $1\cdot10^{-4}$ and constant value (4 significant figures) of the monitored aerodynamic coefficient. To carry out the simulations, a server with Intel Xeon 5630 @ 2.53 GHz (16 processors) CPU, 64 GB RAM memory and 4 TB hard disk

was used that worked under the Windows server 2003 operating system.

2.2 Infrastructure models

In order to analyze the effect of the infrastructure scenarios on the aerodynamic coefficients involved in the rollover of a truck, three stationary ground configurations were proposed for study (see Fig. 1): embankment with downward-slope on the leeward side (type-1 embankment), embankment with upward-slope on the leeward side (type-2 embankment) and flat ground. Height, slope angles and road width have the same dimensions in both embankment scenarios (see Fig. 1). Detailed information about these dimensions as well as about those of the truck can be found in Cheli *et al*. (2011a, b).

To carry out the numerical simulation, the three-dimensional domain representing the regions of air around the truck has to be built (see Fig. 2). The upstream and downstream distances from the bluff bodies (truck and embankment models) in the three scenarios are at least 6Hobs (Hobs being the obstacle height) and 14.4Hobs, respectively (see Fig. 2). The cross section has the same dimensions as the boundary layer test section used in the wind tunnel located in the Polytechnic of Milan: 14 m x 4 m (Bocciolone *et al*. 2008). In addition, the domain was divided into three sub-domains (near domain and two far domains) for several reasons. The near domain surrounding the truck model was defined in order to build a finer grid in this region, which enables the precise capture of the gradients of the flow variables in the proximity of the truck and infrastructures. The remaining domain was divided into two sub domains to set different values in the inlet boundary condition (see Fig. 2).

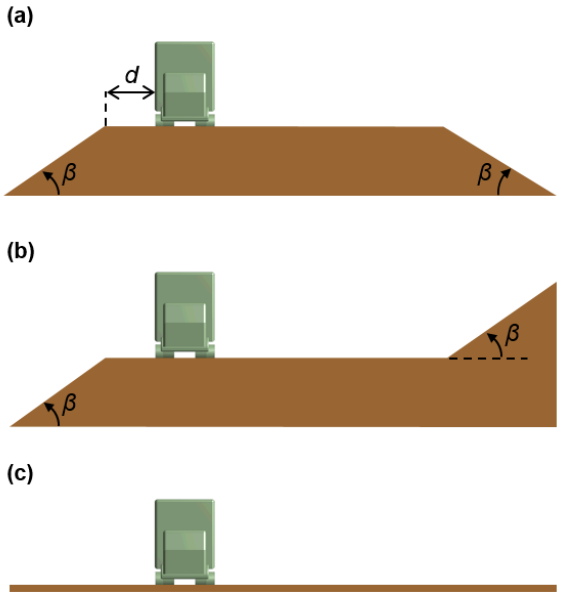

Fig. 1 Truck model located on studied ground configuration: (a) type-1 embankment and (b) type-2 embankment and (c) flat ground

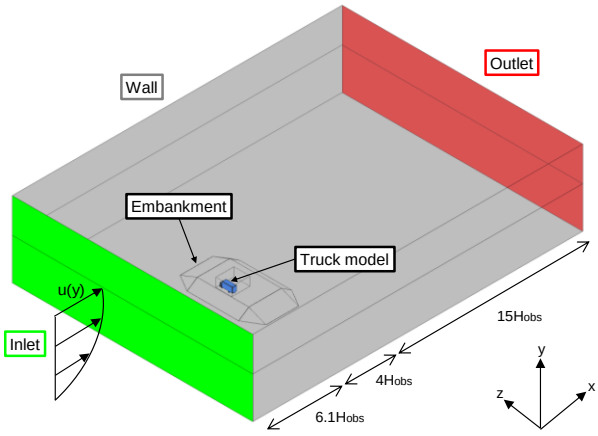

Fig. 2 Geometrical model and boundary conditions used in CFD for type-1 embankment, H_{obs} being the height of obstacle

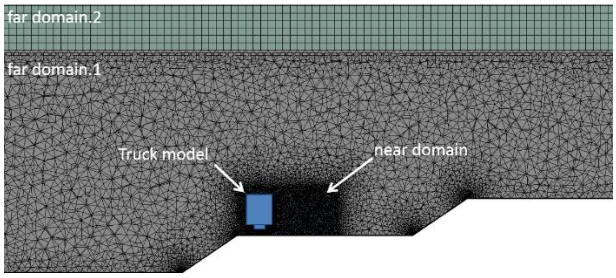

Fig. 3 View of the grid in several regions of the domain for type-2 embankment

2.3 Grid and boundary conditions

Three kinds of grid were used in the CFD models: inflation grid for the regions of fluid close to solid surfaces (infrastructures, walls of test section and truck), tetrahedral grid for far domain.1 and near domain and structural grid for far domain.2 (Fig. 3). The inflation grid enables the high gradients of the variables in the region of the boundary layer to be represented with a greater accuracy. The inflation grid consists of ten inflated layers with a growth rate of 1.2, the thickness of the first layer being calculated to obtain a y^+ value of 1. The variable y^+ is the dimensionless distance from the wall and is calculated as follows

$$y^+ = \frac{u_\tau \cdot y}{\nu} \tag{4}$$

Where y is the distance from the wall; u_τ is the shear velocity; and ν the kinematic viscosity.

The grid size used to solve the CFD models varied from 11.87 million to 20.05 cells for the flat ground and type-1 embankment, respectively. The boundary conditions adopted for solving the numerical model are the following (see Fig. 2) (Tu *et al*. 2012, Madenci and Guven 2015, Yang *et al.* 2017):

- **Inlet**: *U(z)* was defined according to the wind speed

profile introduced in Cheli *et al.* (2011a, b) for low turbulence condition, where the free stream velocity, U_∞, was equal to 13.9 m/s. The components of the wind speed in the Y and Z directions are zero (V,W=0). The fluctuating inflow was generated with the Spectral synthesizer (SS) method proposed by Kraichnan (1970) and modified by Smirnov *et al.* (2001). This method randomly synthesizes a divergence-free velocity field from the summation of Fourier harmonics to generate fluctuations of the velocity components (ANSYS FLUENT 2017). The turbulent length scale l, and the turbulence intensity I, were adjusted to 0.1m and 2%, respectively, as in Cheli *et al.* (2011a, b).

- **Outlet**: Relative pressure p = 0. At the outlet boundary Γ_{out}, the normal gradients of all variables are set to zero, which corresponds to the Neumann boundary condition.
- **Solid walls**: A non-slip condition (U,V,W=0) was adopted at the solid surface of the domain (walls of test section, surfaces of both infrastructures and truck), as seen in Fig. 2.

2.4 Evaluation of aerodynamic loads and moments

The aerodynamic loads and moments acting on the truck are side force (F_S), lift force (F_L) and rollover moment (M_R) (Fig. 4). The side and lift forces acting on the truck were obtained by integrating the pressure distribution over the vertical and horizontal surfaces of truck. On the other hand, the rollover moment was calculated by summation of the moments of side and lift forces around point O (Fig. 4). The aerodynamic force and moment described above were transformed into non-dimensional coefficients by using the following equations:

$$C_S = \frac{F_S}{\frac{1}{2}\rho U^2 A_S}; C_L = \frac{F_L}{\frac{1}{2}\rho U^2 A_S}; C_R = \frac{M_R}{\frac{1}{2}\rho U^2 A_S H} \quad (5)$$

where ρ is the density of the air, 1.18 kg/m^3; A_S is the side area of the truck, 0.189 m^2; H is the reference height, 0.262 m; and U is the mean streamwise wind speed measured at several heights above the ground according to the experimental study by Cheli *et al.* (2011a, b). Particularly, U was measured at the heights of 0.25 m and 0.60 m for the flat ground and embankment infrastructures, respectively.

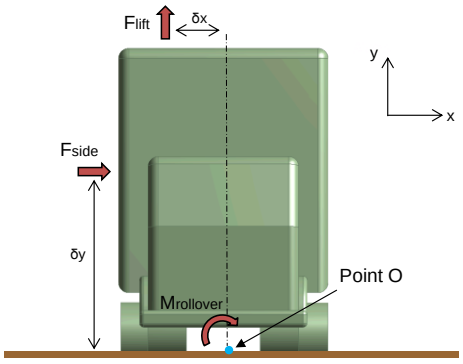

Fig. 4 Aerodynamic loads responsible for the rollover moment acting on the full-scale truck

2.5 Design of experiments (DOE) methodology

The influence on the aerodynamic behavior of the truck of variables such as the slope angle β of the type-1 embankment and the horizontal distance d between the edge of the embankment slope and the truck (See Fig. 1), were studied by means of a DOE. The type-1 embankment was used for analysis instead of the type-2 because of its more unfavorable influence on the vehicle stability, as can be seen in section 3.2. The first step in the DOE procedure (Del Coz Díaz *et al.* 2012, Telenta *et al*. 2015) consists of selecting a method to determine the number of cases to run and the values of the input variables for these cases. In this case, the Central Composite Design (CCD) method was selected and then the different combinations of input values were considered to obtain the predefined output variables.

The Response Surface models (RS-models) were developed based on the second order polynomial regression models chosen as an approximation technique along with the results obtained from the DOE method. As a part of the Response Surface Methodology (RSM), the input variables $x_1, x_2 \ldots, x_n$ must be coded to compare their effects on truck stability. Factors vary between -1 and +1, which corresponds to a variation between a minimum and a maximum value in the coded scale, respectively. The second-order models obtained during the RSM enable the identification of the critical points (maximum, minimum, or saddle) and can be expressed in a general form as (Montgomery 2001)

$$\hat{Y} = \alpha_0 + \sum_{i=1}^{n} \alpha_i x_i + \sum_{i=1}^{n} \alpha_{ii} x_i^2 + \sum_{i<j}^{n} \alpha_{ij} x_i x_j \quad (6)$$

where $\hat{Y}$ is the predicted response variable; x_i denotes the coded values of the input variables; α_0, α_i, α_{ii}, α_{ij} indicate the regression coefficients (offset term, main, quadratic and interaction effects); and n is the number of variables studied. The regression coefficients are determined by the Ordinary Least Squares (OLS) method. The OLS estimator is defined according to the following expression (Montgomery 2001, Del Coz Díaz *et al.* 2011)

$$\vec{\alpha}_{OLS} = \left(\vec{X}^T \vec{X}\right)^{-1} \vec{X}^T \vec{Y} \quad (7)$$

where $\vec{\alpha}_{OLS}$ is a vector of regression coefficients; $\vec{X}$ is an extended designed matrix for the input variables including the coded levels; and $\vec{Y}$ is a column vector of response variables that includes the numerical simulation results for the combinations of input variable values previously proposed by the DOE method. The input variables with their variation ranges (maximum, minimum and current value) as well as the output variables, are shown in Table 1. Finally, an optimization of the input variables was carried out by means of identifying the combination of input variables values that minimized or maximized a given objective function.

Table 1 Ranges of input variables and response variables used in the DOE analyses

Input variables	β^a (°)	d^b (mm)
Maximum	53	180
Minimum	15	30
Current	34	105
Output variables	*Cf_Side* *Cf_Lift*	*Cm_Rollover*

[a]Angle of the type-1 embankment slope with the horizontal plane (see Fig. 1).
[b]Distance between the edge of the type-1 embankment slope and truck in full scale (see Fig. 1).

3. Results and discussion

3.1 Reynolds number effect on aerodynamic response

In order to correctly obtain the aerodynamic loads acting on the full-scale truck, it is necessary that the dynamic similarity between the 1/10 scaled-down truck model and the full-scale truck is fulfilled. To satisfy the dynamic similarity criterion, the magnitudes of the Reynolds number Re, analyzed during the numerical simulation of the 1/10 scaled-down truck model should be equal to the full-scale truck case (Cermak and Isyumov 1998, Kang and Lee 2008). Therefore, to obtain the same value of *Re*, the wind speed should be 10 times the actual wind speed in the numerical simulation. None information about the fulfillment of the dynamic similarity criterion was indicated in Cheli *et al.* (2011a, b) so it was found interesting to check it in this section. Accordingly, the independence between the aerodynamic coefficients of the truck model and the *Re* values was assessed, since the actual wind velocity for the full scale truck was unknown.

For this study, flat ground was selected, because the part of the speed profile that influences the truck model does so at lower values of *Re* in this infrastructure. The aerodynamic coefficients of the truck model under cross wind conditions (yaw angle of 90º) were obtained for five magnitudes of *Re* between 2.5×10^5 and 7.2×10^5. The range of *Re* values proposed in this study includes the value used in the experimental tests. The Re values were obtained by using the following expression

$$\mathrm{Re}=\frac{\rho U_\infty L}{\mu} \tag{8}$$

where U_∞ is the undisturbed wind speed and L is the characteristic linear dimension whose value is equal to the reference height value defined for the aerodynamic coefficients. The aerodynamic coefficients of the truck model showed small variations in the range analyzed, as seen in Fig. 5. As the minimum value of Reynolds number defined in the numerical simulation for the studied scenarios was 2.5×10^5, it can be assumed that the dynamic similarity requirement is satisfied.

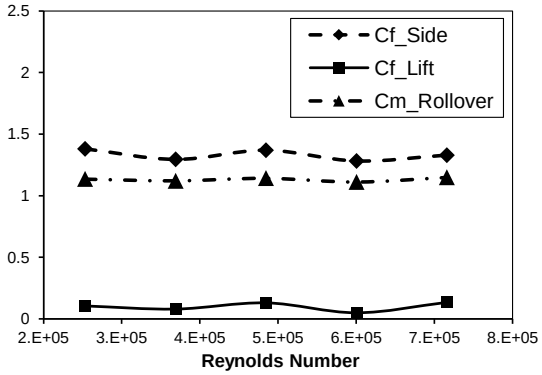

Fig. 5 Relationship between the Reynolds number and the aerodynamic coefficients of truck model under cross wind conditions

3.2 Influence of the embankment type

In order to analyze the influence of the embankment type on the stability of a truck model, the aerodynamic coefficients of a truck were determined for flat ground, an embankment with downward-slope on the leeward side (type-1 embankment) and an embankment with upward-slope on the leeward side (type-2 embankment) (see Fig. 6).

The rollover moment is the key coefficient when the risk of suffering a rollover accident under cross wind conditions (Schober *et al*. 2010) has to be evaluated; accordingly, the results indicate that the embankments affect the truck stability more negatively than flat ground (see Fig. 6). This could be due to the slope of the two embankments located on the upward side of the truck, because the slope causes a decrease in the distance between the streamlines and consequently the air flow speed increases (see Fig. 7). Specifically, the maximum velocity of the air flow is reached at the end of the upward slope for both types of embankments. Therefore, the greatest differences in pressure between the windward side and the leeward side of the truck are found for the embankments (see Fig. 8). The most significant relative differences between the experimental reference values and those from the numerical simulation were found for the lift aerodynamic coefficient (see Fig. 6). However, in general, the aerodynamic coefficients obtained through both techniques suggest the same conclusions regarding the infrastructures having a more detrimental influence on the vehicle stability under cross wind conditions, as shown in Fig. 6.

A higher value of the rollover coefficient was obtained for the type-1 embankment than for the type-2 embankment. This is because the slope of the type-2 embankment on the leeward side of the truck can slow down the wind speed in the air region between the truck and this slope (Fig. 8). Therefore, the relative pressure values are closer to zero and as a consequence, the suction force acting on the leeward surface of the truck is less on the type-2 embankment. Regarding the lift coefficient, the small differences in pressure between the top and the bottom of the truck for all the infrastructures are in agreement with the positive low values obtained for the lift coefficient shown in Fig. 6.

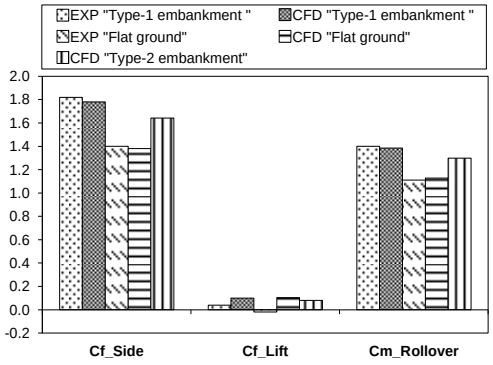

Fig. 6 Comparison of aerodynamic coefficients with perpendicular wind (γ=90º), obtained through wind tunnel tests (EXP) by Cheli *et al*. (2011b) and numerical modeling (CFD)

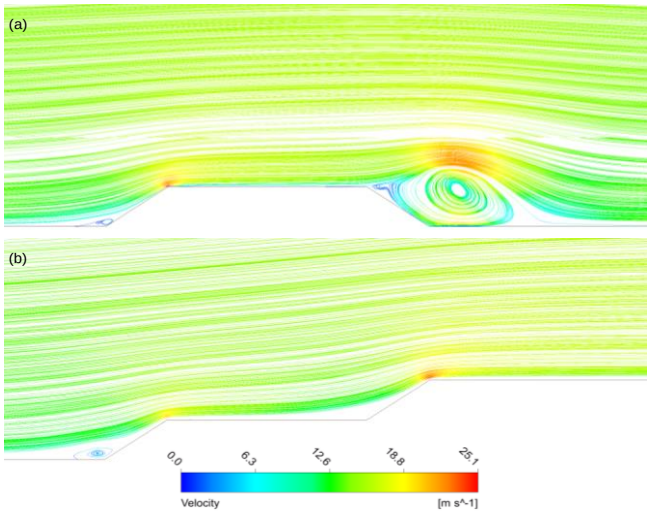

Fig. 7 Streamlines of velocity field around: (a) the type-1 embankment; and (b) the type-2 embankment

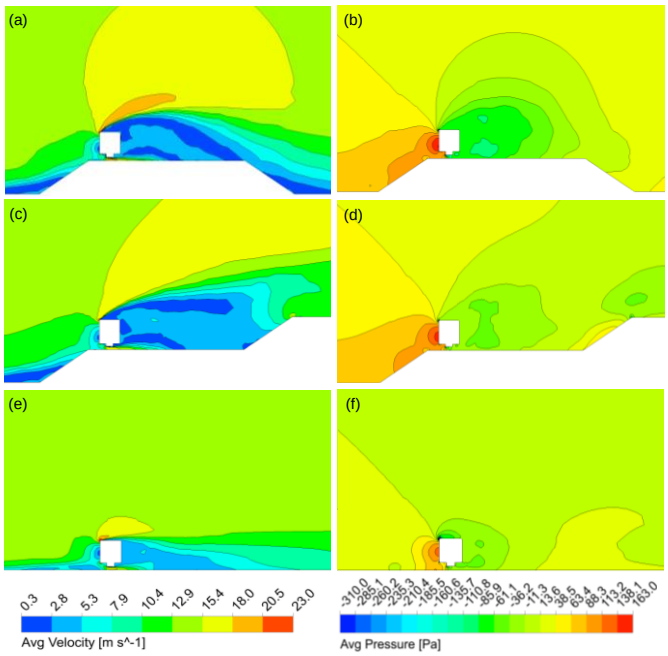

Fig. 8 Mean pressure and velocity contours calculated from the numerical simulation results for the: type-1 embankment (a) and (b); type-2 embankment (c) and (d); and flat ground (e) and (f)

3.3 Effect of the slope angle and the truck's position

During the DOE analysis, 9 numerical models were solved in order to determine the surface response models. Figs. 9(a)-9(c) indicate the maximum variation undergone by the aerodynamic coefficients of the truck studied as a function of the truck's position on the road, and the slope angle, for the type-1 embankment (see Fig. 1). All the aerodynamic coefficients are sensitive to variations both in the truck's position on the road and the slope angle (see Fig. 9). Particularly, a negative correlation exists between the aerodynamic coefficients and the truck's position on road *d*.

The increase in the aerodynamic coefficients with the decrease in the distance between the truck and the embankment slope located on the windward side is due to the accelerated streamlines from the slope that hit a greater side surface of truck and flow closer to the top surface of truck.

On the other hand, the relationships between the aerodynamic coefficients and the slope angle are similar for the rollover moment and side force, but not for the lift force.

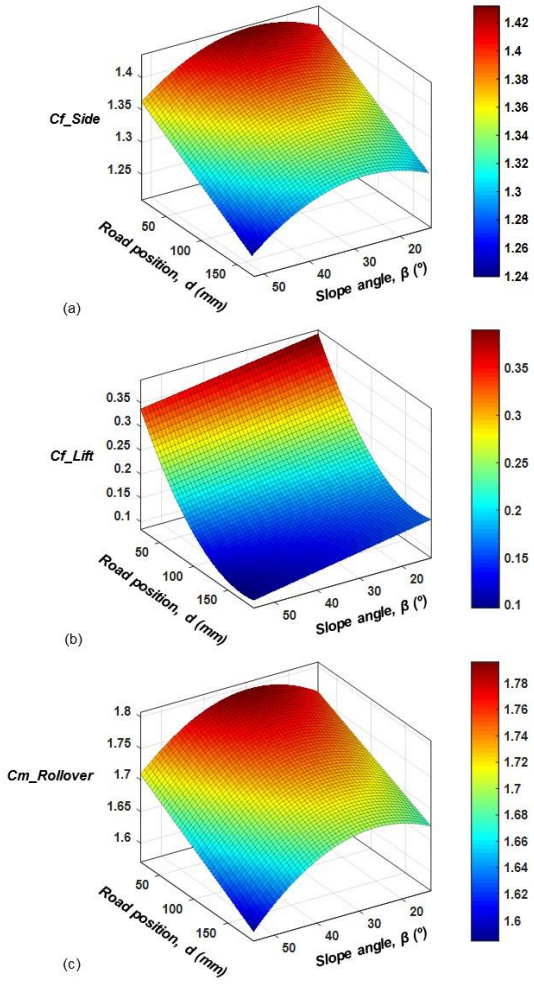

Fig. 9 Response surfaces of the truck's position on the road and the slope angle versus the aerodynamic coefficients of the truck: (a) side force, (b) lift force; and (c) rollover moment

In the case of the lift force, an increase in slope angle diminishes the coefficient whereas, in the case of the rollover moment and side force, the coefficients firstly increase with higher values of slope angle and then diminish (see Fig. 9). An increase in the slope angle moves the streamlines away from the top surface of the truck, and as a consequence, the lift force decreases. In addition, this increase of slope angle can accelerate the flow lines, narrowing the distance between them (see Fig. 7) and in turn allowing the increase in the side and rollover coefficients. However, these coefficients can also decrease at the highest values of the slope angle studied due to the streamlines from the slope hitting a smaller side surface of the truck. Therefore, both the side force and rollover moment versus slope angle may exhibit different trends depending on the range of the slope angle values studied, as shown in Fig. 9.

A lower risk a rollover accident is expected when an appropriate combination of input variables minimizes the rollover moment coefficient. Thus, the minimum rollover coefficient is 1.23 and it is obtained for a truck position on the road of 180 mm (1800 mm in full scale) and a slope angle of 53º. Meanwhile, the worst combination of values from a rollover perspective was obtained for a truck position on the road of 30 mm (300 mm in full scale) and a slope angle of 27.7º.

4. Conclusions

In this work, several numerical simulations were carried out to analyze the relationships between the aerodynamic coefficients of a truck and the type of road infrastructure. In addition, the effect of both the slope angle of an embankment and the truck position on the road on the aerodynamic response of the truck was studied. The main findings from the results are summarized as follows:

- Flat ground is the infrastructure where the rollover coefficient acting on the truck model shows the lowest values under cross wind conditions (yaw angle of 90º), while the highest values were obtained for the type-1 embankment.

- A negative sensitivity of the rollover moment coefficient with respect to the truck's position on the road has been found. However, the sensitivity of the rollover moment coefficient to the slope angle can be negative or positive depending on the range of slope angle values considered.

- The good agreement between the experimental and numerical results demonstrates that the LES approach in combination with the Finite Volume Method is a suitable methodology to estimate the vehicle's aerodynamic response.

- The values of the truck's position on the road and the slope angle that optimize the vehicle stability were

determined by applying the Response Surface Methodology.

- The dynamic similarity between the 1/10 scaled-down truck model and a full-scale model can be considered to have been fulfilled according to the existing relationship between the aerodynamic coefficients and the Reynolds number.

- The DOE procedure, when applied on a validated model, enables the saving of time and costs when manufacturing prototypes and carrying out field testing.

Acknowledgments

This work was supported by the OASIS Research Project, that was co-financed by the CDTI under the Ministry of Economy, Industry and Competitiveness) and developed by 16 Spanish companies: Iridium, OHL Concesiones, Abertis, Sice, Indra, Dragados, OHL, Geocisa, GMV, Asfaltos Augusta, Hidrofersa, Eipsa, PyG, CPS, AEC and Torre de Comares Arquitectos S.L; and 16 research centres. The authors would also like to thank the GICONSIME research group of the University of Oviedo (Spain) for their collaboration in this research. The authors also acknowledge the partial funding with FEDER funds under the Research Project FC-15-GRUPIN14-004.

References

Alvarez-Legazpi, P., Vargas-Muñoz, M., Martínez-Acevedo, J.C., Botella-Malagón, J. and Rodríguez- Fernández, M. (2010), "Cross wind protection systems for high speed Railway Lines", *Proceedings of the ASME Joint Rail Conference 2010, JRC2010*, April 27–29, 2010, Urbana, Illinois, USA.

ANSYS Inc. *Fluent Manual Release 17.0.* (2017), Canonsburg, PA, USA.

Andersson, B., Andersson, R., Hakansson, L., Mortensen M., Rahman S. and Berend V.W. (2012). *Computational fluid dynamics for engineers*, Cambridge University Press, New York, USA.

Argentini, T., Ozkan, E., Rocchi, D., Rosa, L. and Zasso, A. (2011), "Cross-wind effects on a vehicle crossing the wake of a bridge pylon", *J. Wind Eng. Ind. Aerod*., **99(6-7)**, 734-740.

Baker, C.J. and Reynolds, S. (1992), "Wind-induced accidents of road vehicles", *Accid. Ana. Prev*., **24**(6), 559-575.

Bettle, J., Holloway, A.G.L. and Venart, J.E.S. (2003), "A computational study of the aerodynamic forces acting on a tractor-trailer vehicle on a bridge in cross-wind", *J. Wind Eng. Ind. Aerod*., **91**(5), 573-592.

Bitsuamlak, G.T., Stathopoulos, T. and Bédard, C. (2004), "Numerical evaluation of wind flow over complex terrain: Review", *J. Aerospace Eng*., **17**(4), 135-145.

Bocciolone, M., Cheli, F., Corradi, R., Muggiasca, S. and Tomasini, G. (2008), "Crosswind action on rail vehicles: Wind tunnel experimental analyses", *J. Wind Eng. Ind. Aerod*., **96**(5), 584-610.

Cermak, J.E. and Isyumov, N. (1998), *Wind Tunnel Studies of Buildings and Structures.* ASCE, Reston, Virginia.

Cheli, F., Corradi, R., Rocchi, D., Tomasini, G. and Maestrini, E. (2010), "Wind tunnel tests on train scale models to investigate the effect of infrastructure scenario", *J. Wind Eng. Ind. Aerod*., **98**(6-7), 353-362.

Cheli, F., Corradi, R., Sabbioni, E. and Tomasini, G. (2011), "Wind tunnel tests on heavy road vehicles: Cross wind induced loads-Part 1", *J. Wind. Eng..Ind. Aerod*., **99**(10), 1000-1010.

Cheli, F., Ripamonti, F., Sabbioni, E. and Tomasini, G. (2011), "Wind tunnel tests on heavy road vehicles: Cross wind induced loads-Part 2", *J. Wind Eng. Ind. Aerod.*, **99**(10), 1011-1024.

Coleman, S.A. and Baker, C.J. (1990, "High sided road vehicles in cross winds", *J. Wind Eng. Ind. Aerod*., **36**(1-3), 1383-1391.

Del Coz Díaz, J.J., García Nieto, P.J., Castro-Fresno, D. and Menéndez Rodríguez, P. (2011), "Steady state numerical simulation of the particle collection efficiency of a new urban sustainable gravity settler using design of experiments by FVM", *Appl. Math. Comput*., **217**(21), 8166-8178.

Del Coz Díaz, J.J., Serrano López, M.A., López-Colina Pérez, C. and Álvarez Rabanal, F.P. (2012), "Effect of the vent hole geometry and welding on the static strength of galvanized RHS K-joints by FEM and DOE", *Eng. Struct*., **41**, 218-233.

Delaunay, D., Baker, C.J., Cheli, F., Morvan, H., Berger, L., Casazza, M., Gomez, C., Cleac'h C.Le., Saffell, R., Grégoire, R. and Vinuales, A. (2006), "Development of wind alarm systems for road and rail vehicles: presentation of the WEATHER project", *Proceedings of the SIRWEC2006, 13th International Riad Weather Conference*, Torino, Italy.

Diedrichs, B., Sima, M., Orellano, A. and Tengstrand, H. (2007). "Crosswind stability of a high-speed train on a high embankment", *Proc. Inst. Mech. Eng. Pt. F: J. Rail Rapid Transit*, **221**(2), 205-225.

Dorigatti, F., Sterling, M., Rocchi, D., Belloli, M., Quinn, A.D., Baker, C.J. and Ozkan, E. (2012), "Wind tunnel measurements of crosswind loads on high sided vehicles over long span bridges", *J. Wind Eng. Ind. Aerod*., **107-108**, 214-224.

Dragomirescu, E., Wang, Z. and Hoftyzer, M.S. (2016), "Aerodynamic characteristics investigation of Megane multi-box bridge deck by CFD-LES simulations and experimental tests", *Wind Struct.*, **22**(2), 161-184.

European Research Community on Flow, Turbulence and Combustion (ERCOFTAC). *Special Interest Group on Quality and Trust in Industrial CFD Best Practice Guidelines*, (2000), (Eds. M. Casey and T. Wintergerste), (online).

García, J., Muñoz-Paniagua, J., Jiménez, A., Migoya, E. and Crespo, A. (2015), "Numerical study of the influence of synthetic turbulent in flow conditions on the aerodynamics of a train", *J. Fluid. Struct*., **56**, 134-151.

He, X., Shi, K., Wu, T., Wang, H. and Qin, H (2016), "Aerodynamic performance of a novel wind barrier for train-bridge system", *Wind Struct*., **23**(3), 171-189.

Hibino, Y., Shimomura, T. and Tanifuji, K. (2010), "Full-scale experiment on the behavior of a railway vehicle being subjected to lateral force", *J. Mech. Syst. Transp. Logist*., **3**, 35-43.

Hoppmann, U., Koenig, S., Tielkes, T. and Matschke, G. (2002), "A short-term strong wind prediction model for railway application: Design and verification", *J. Wind Eng. Ind. Aerod*., **90**(10), 1127-1134.

Imai, T., Fujii, T., Tanemoto, K., Shimamura, T., Maeda, T., Ishida, H. and Hibino, Y. (2002), "New train regulation method based on wind direction and velocity of natural wind against strong winds", *J. Wind Eng. Ind.Aerod.*, **90**(12-15), 1601-1610.

Kang, J.H. and Lee, S.J. (2008), "Experimental study of wind load on a container crane located in a uniform flow and atmospheric boundary layers", *Eng. Struct*., **30**(7), 1913-1921.

Kraichnan, R.H. (1970), "Diffusion by a random velocity field", *Phys Fluids*, **13**(1), 22-31.

Ma, L., Zhou, D., Han, W., Wu, J. and Liu, J. (2016), "Transient aerodynamic forces of a vehicle passing through a bridge

tower's wake region in crosswind environment", *Wind Struct*., **22**(2), 211-234.
Madenci, E. and Guven, I. (2015), *The Finite Element Method and Applications in Engineering Using ANSYS*. Springer, New York.
Miao, X.J., Tian, H.Q. and Gao, G.J. (2010), "Effect of railway environment on aerodynamic performance of train on embankment", *Zhongnan Daxue Xuebao (Ziran Kexue Ban)/Journal of Central South University (Science and Technology)*, **41**(5), 2028-2033.
Montgomery, D.C. (2001), *Design and Analysis of Engineering Experiments*. John Wiley & Sons, New York.
Patankar, S.V. and Spalding, D.B. (1972), "A calculation procedure for heat, mass and momentum transfer in three-dimensional parabolic flows", *Int. J. Heat Mass Transf*., **15**(10): 1787-1806.
Schober, M., Weise, M., Orellano, A., Deeg, P. and Wetzel, W. (2010), "Wind tunnel investigation of an ICE 3 endcar on three standard ground scenarios", *J. Wind Eng. Ind. Aerod*., **98**(6-7), 345-352.
Shao, X.M., Wan, J., Chen, D.W. and Xiong, H.B. (2011), "Aerodynamic modeling and stability analysis of a high-speed train under strong rain and crosswind conditions", *J. Zhejiang University: Science A*. **12**(12), 964-970.
Smagorinsky, J. (1963), "General circulation experiments with the primitive equations: I The basic experiment", *Mon Weather Rev*., **91**, 99-164.
Smirnov, R., Shi, S. and Celik, I. (2001), "Random flow generation technique for large eddy simulations and particle-dynamics modelling", *J. Fluids Eng*., **123**, 359-371.
Sterling, M., Quinn, A.D., Hargreaves, D.M., Cheli, F., Sabbioni, E., Tomasini, G., Delaunay, D., Baker, C.J. and Morvan, H. (2010), "A comparison of different methods to evaluate the wind induced forces on a high sided lorry", *J. Wind Eng. Ind. Aerod*., **98**(1), 10-20.
Suzuki, M., Tanemoto, K. and Maeda, T. (2003), "Aerodynamic characteristics of train/vehicles under cross winds", *J. Wind Eng. Ind. Aerod*., **91**(1-2), 209-218.
Telenta, M., Batista, M., Biancolini, M.E., Prebil, I. and Duhovnik, J. (2015), "Parametric numerical study of wind barrier shelter", *Wind Struct*., **20**(1), 75-93.
Tsubokura, M., Nakashima, T., Kitayama, M., Ikawa, Y., Hee-Doh, D. and Kobayashi, T. (2010), "Large eddy simulation on the unsteady aerodynamic response of a road vehicle in transient crosswinds", *Int. J. Heat Fluid Flow*., **31**(6), 1075-1086.
Tu, J., Yeoh, G.H. and Liu, C. (2012), *Computational Fluid Dynamics*. *A Practical Approach*, 2nd Ed., Butterworth-Heinemann, Oxford.
Wang, B., Xu, Y.L., Zhu, L.D. and Li, Y.L. (2014), "Crosswind effect studies in road vehicle passing by bridge tower using computational fluid dynamics", *Eng. Appl. Comput. Fluid Mech*., **8**(3), 330-344.
Wu, M., Li, Y. and Zhang, W. (2017), "Impacts of wind shielding effects of bridge tower on railway vehicle running performance", *Wind Struct*., **25**(1), 63-77.
Yang, Y., Xie, Z. and Gu, M. (2017), "Consistent inflow boundary conditions for modelling the neutral equilibrium atmospheric boundary layer for the SST k-ω model", *Wind Struct*., **24**(5), 465-480.
Yang, S., Xiang, H., Fang, C., Wang, L. and Li, Y. (2017), "Wind tunnel tests on flow fields of full-scale railway wind barriers", *Wind Struct*., **24**(2), 171-184.